A measurement of the muon-induced neutron yield in lead at a depth of 2850 m water equivalent

L. Reichhart[*,†], A. Lindote[**], D.Yu. Akimov[‡], H.M. Araújo[§], E.J. Barnes[*],
V.A. Belov[‡], A. Bewick[§], A.A. Burenkov[‡], V. Chepel[**], A. Currie[§], L. DeViveiros[**],
B. Edwards[¶], V. Francis[¶], C. Ghag[*,†], A. Hollingsworth[*], M. Horn[§], G.E. Kalmus[¶],
A.S. Kobyakin[‡], A.G. Kovalenko[‡], V.A. Kudryavtsev[‖], V.N. Lebedenko[§],
M.I. Lopes[**], R. Lüscher[¶], P. Majewski[¶], A.St J. Murphy[*], F. Neves[**], S.M. Paling[¶],
J. Pinto da Cunha[**], R. Preece[¶], J.J. Quenby[§], P.R. Scovell[*], C. Silva[**],
V.N. Solovov[**], N.J.T. Smith[¶], P.F. Smith[¶], V.N. Stekhanov[‡], T.J. Sumner[§],
C. Thorne[§] and R.J. Walker[§]

[*] *School of Physics & Astronomy, SUPA University of Edinburgh, UK*
[†] *High Energy Physics Group, Department of Physics & Astronomy, University College London, UK*
[**] *LIP–Coimbra & Department of Physics of the University of Coimbra, Portugal*
[‡] *Institute for Theoretical and Experimental Physics, Moscow, Russia*
[§] *High Energy Physics Group, Blackett Laboratory, Imperial College London, UK*
[¶] *Particle Physics Department, STFC Rutherford Appleton Laboratory, Chilton, UK*
[‖] *Department of Physics & Astronomy, University of Sheffield, UK*

Abstract. We present results from the measurement of the neutron production rate in lead by high energy cosmic-ray muons at a depth of 2850 m water equivalent (mean muon energy of 260 GeV). A tonne-scale highly segmented plastic scintillator detector was utilised to detect both the energy depositions from the traversing muons as well as the delayed radiative capture signals of the induced neutrons. Complementary Monte Carlo simulations reproduce well the distributions of muons and detected muon-induced neutrons. Absolute agreement between simulation and data is of the order of 25%. By comparing the measured and simulated neutron capture rates a neutron yield in pure lead of $(5.78^{+0.21}_{-0.28}) \times 10^{-3}$ neutrons/muon/(g/cm^2) has been obtained.

Keywords: Muon-induced neutron background, cosmic-ray muons, neutrons, underground experiments, ZEPLIN–III, dark matter, GEANT4, Monte Carlo simulations
PACS: 25.40.Lw, 98.70.Vc, 24.10.Lx, 25.30.Mr

INTRODUCTION

Despite the efforts of rare event searches to go deep underground, there remains a finite background of cosmic-ray muons energetic enough to penetrate through the full rock overburden of any given underground laboratory. These may then produce high energy neutrons in the surrounding rock as well as in the actual shielding of the experiments. As improved sensitivity of rare event search experiments is achieved, precise measurements and mitigation of the muon-induced neutron background in different materials become a high priority task. Careful assessment also helps in benchmarking Monte Carlo simulations, which guide the design of future detectors and their mandatory veto systems.

A large neutron production rate is observed for high-A materials. As such, the production yield in lead is greatly enhanced in comparison to other common shielding materials. Nevertheless, several rare event search projects utilise large amounts of lead to shield against the ambient γ-ray background. Thus, the evaluation of the muon-induced neutron production rate in this material is of special interest.

Here we present a summary of the muon-induced neutron yield in lead measured from the data accrued with the highly segmented anti-coincidence detector installed around the ZEPLIN–III dark matter instrument. The measurement was conducted in parallel to the 319-day long second science run of the experiment in 2010/11. For a more detailed discussion of this measurement and the complementary Monte Carlo simulation the reader is referred to Ref. [1].

SETUP

The ZEPLIN–III instrument [2] is a dual phase liquid/gas xenon detector, built to observe low-energy nuclear recoils resulting from elastic scattering of weakly interacting massive particles (WIMPs). The final scientific exploitation of the long-running ZEPLIN dark matter project at the Boulby Underground Laboratory achieved cross-section limits for scalar WIMP–nucleon and spin-dependent WIMP–neutron channels of 3.9×10^{-8} pb and 8.0×10^{-3} pb near a WIMP mass of 50 GeV/c^2 (90% confidence level), respectively [3, 4]. For the second science run the detector was upgraded with a 1-tonne plastic scintillator anti-coincidence detector (the 'veto'), mounted around the main instrument [5].

The 15 cm thick veto system consists of 52 individual polystyrene-based plastic scintillator UPS-923A (p-terphenyl 2%, POPOP 0.02%) modules, each equipped with a single PMT (ETEL-9302 KB), forming a barrel (built from 32 sections of $\sim$1 m in length) and a roof (built from 20 sections of different lengths to form a near-circular shape). It surrounds a 15 cm thick Gd-loaded polypropylene shielding, which in turn encircles the ZEPLIN–III instrument. This entire structure is then enclosed in a 20 cm thick lead castle. For a detailed description of the design of each individual component, the full setup and the overall performance of the veto see Refs. [5, 6].

Monte Carlo simulations

Simulated primary muon energy spectra and angular distributions were obtained by propagating atmospheric muons from the Earth's surface through the rock overburden of the Boulby Underground Laboratory [7] using the MUSIC code [8, 9]. Subsequently, this distribution was sampled with the MUSUN code [9, 10] on the surface of a virtual cuboid enclosing the main laboratory cavern and at least 5 m of additional rock on each side. The sampled muons were then propagated using GEANT4 [11] version 9.5 with the modular physics list `Shielding` implemented. Additionally, thermal scattering cross-sections for neutrons scattering off chemically bound atoms were added (below 4 eV). The output generated by the simulation has been designed to recreate the conditions of the experiment, *i.e.* a waveform-like readout with a resolution of 0.1 μs for all 52 individual channels separately. Thus, direct comparison to data as well as the use of equivalent analysis cuts for experimental and simulated data was possible.

MUON EVENT SELECTION

An anti-coincidence device for a dark matter experiment needs to provide maximum sensitivity to low energy depositions from multiply scattering radioactivity neutrons and γ-rays. Consequently, the large energy depositions from muons traversing the scintillator bars result in heavily saturated pulses. Selection of muons from this data set was therefore non-trivial, but was achieved by searching for coincident highly saturated signals in roof and barrel scintillators. Equivalent selection cuts were used on the Monte Carlo generated data. Figure 1 shows a comparison of event distributions between pairs of roof modules and barrel modules from experimental data and simulations. Despite the complex structure of module coincidences, due to the relative orientation of the scintillator bars featuring different response functions, the experimental data is well reproduced by the Monte Carlo and, as such, confirms that the selected experimental data correspond to cosmic-ray muon events.

A rate of 32.3±0.4 muons/day was measured. Using the normalised flux through a sphere in the simulation, a muon flux of $(3.75\pm0.09) \times 10^{-8}$ muons/s/cm^2 was deduced from the comparison between simulated and experimental measured rates. This result is in excellent agreement with the last reported value for the muon flux in the Boulby Underground Laboratory of $(3.79\pm0.15) \times 10^{-8}$ muons/s/cm^2 [12].

MUON-INDUCED NEUTRON YIELD

In this experimental setup muon-induced neutrons were predominantly produced in the $\sim$60-tonne lead shield, enclosing the entire structure to protect the experiment from ambient γ-rays. For the determination of the muon-induced neutron yield in lead we counted the number of neutrons captured in the veto following a recorded muon event. This was then compared with simulations performed using the same analysis cuts. Neutrons were identified through the delayed γ-rays emitted following neutron capture and detected in one or more scintillator modules simultaneously.

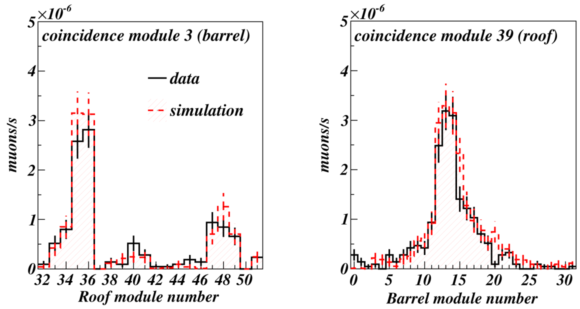

FIGURE 1. (Colour online) Sample of coincident pairs of modules for selected muon events, showing coincidences from a barrel slab (left, module 3) and a roof slab (right, module 39) with all modules of the roof and the barrel, respectively. The simulation, scaled to the total muon rate observed in the data, is shown by the red dashed histogram in comparison to the data (black solid histogram).

Selection cuts for time coincident signals (within $\pm 0.2\ \mu$s of each other) coming from different scintillator modules, have been defined to optimise the detected neutron event rate and simultaneously minimise detection of spurious signals due to afterpulses and accidental coincidences of γ-ray events. A global threshold was set such that regardless of the number of scintillators fired in coincidence, all events must have a total signal size of at least 8 phe, except for single scintillator events. In this case a minimum threshold of 10 phe had to be fulfilled. Additional minimum thresholds have also been set for each of the pulses contributing to higher multiplicity neutron events; for more details see Ref. [1]. In the experimental data, an overall mean of 0.346 ± 0.007 (stat.) ${}^{+0.000}_{-0.014}$ (syst.) neutrons (including background corrections) was observed for every muon detected. The systematic error covers the uncertainty in the correlation of spurious signals with the large energy depositions from the traversing muons. The expected total muon-induced neutron rate calculated from simulations is 0.275 ± 0.003 (stat.) ${}^{+0.004}_{-0.007}$ (syst.) neutrons/muon. Here, the systematic errors were calculated from the variability in the energy calibration. The total yield from the data exceeds the simulation by ∼26%. Despite the difference in the absolute rates, when comparing data to normalised spectra from the simulation excellent agreement is demonstrated. Figures 2 (a)–(c) show the time delay distribution for detected neutrons, the module multiplicity per neutron event and the energy depositions associated with the observed (captured) neutrons in the region before the onset of saturation for experimental and normalised simulated data, respectively. Figure 2 (d) shows the relative fraction of observed neutrons per muon for data and simulation. When exploring neutron multiplicities, rather than scaling the simulation to the total number of neutrons observed in the data, a simple normalisation to the number of detected muons has been applied.

The productions sites of the generated neutrons were determined from the Monte Carlo simulations. For this specific experimental setup a relative fraction of ∼95% of detected capture neutrons has been produced in the surrounding lead shielding. Thus, the observed neutron rate may be used to derive an absolute neutron production yield in this material. To do so an idealised simulation of neutron production by a mono-energetic beam of muons in pure lead was performed, following the methodology in Refs. [12, 13], and subsequently scaled by the ratio in rate observed between the data and the full detector simulation. A production rate of $(4.594 \pm 0.004) \times 10^{-3}$ neutrons/muon/(g/cm^2) was obtained from simulations with the simplified geometry for pure lead. The experimental muon-induced neutron rate was found to be a factor of ∼1.26 higher. As such, our results suggest a true production rate in lead by 260 GeV muons of $(5.78^{+0.21}_{-0.28}) \times 10^{-3}$ neutrons/muon/(g/cm^2), assuming neutron transport and detection were modelled accurately.

CONCLUSION

Accurate data on the muon-induced neutron yield of the materials present in the surroundings, shieldings and instruments of rare event searches are of great importance for the development and design of next generation experiments. The knowledge of absolute rates in conjunction with the ability to simulate these processes using Monte Carlo simulation techniques allow for an accurate determination of the irreducible background in these searches. This is of special interest for direct dark matter search experiments.

Here, we presented the measurement of the muon-induced neutron yield in pure lead performed with the veto of the ZEPLIN–III experiment, resulting in $(5.78^{+0.21}_{-0.28}) \times 10^{-3}$ neutrons/muon/(g/cm^2) for a mean muon energy of 260 GeV.

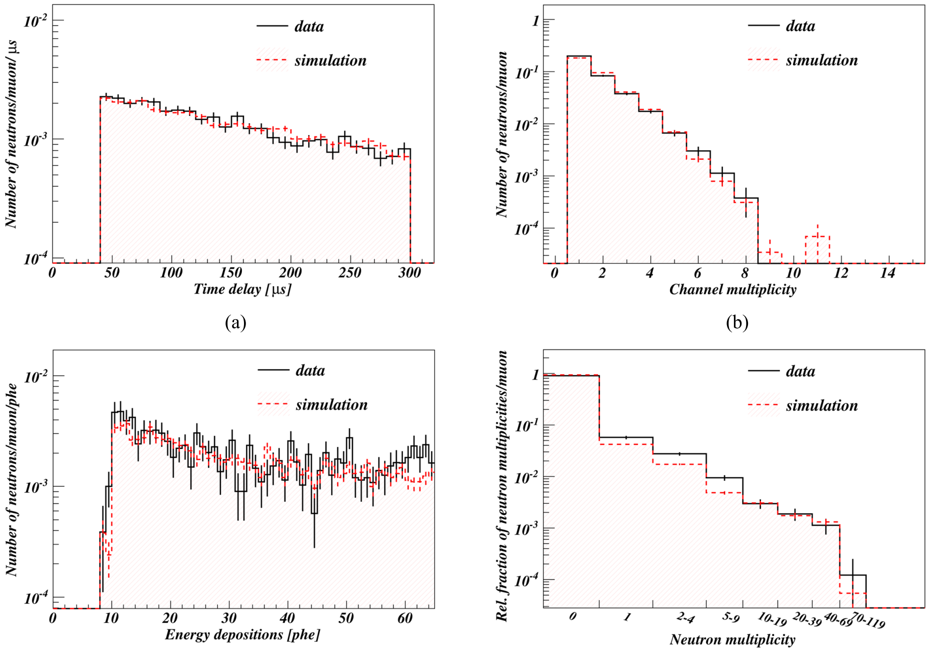

(a) (b)

(c) (d)

FIGURE 2. (Colour online) Histograms of detected capture neutrons comparing background corrected experimental data (black solid) and simulations (red dashed) — the results from simulations in part (a–c) are normalised to the total number of neutrons observed in the data — showing: (a), the time delay distributions; (b), the channel (scintillator module) multiplicities; (c), the energy depositions below the saturation point in the data with single photoelectron resolution (1 phe $\simeq$ 20 keV); and, (d), the relative fractions of neutron multiplicities per muon, *i.e.* the number of delayed signals observed after a muon trigger in the defined time window normalised to the total number of observed muons in each case.

ACKNOWLEDGMENTS

Support is acknowledged from the Science & Technology Facilities Council (ST/K006436/1, ST/K003178/1, ST/K003208/1, ST/K006428/1, ST/K003186/1, ST/K006444/1, ST/K006770/1), Cleveland Potash Ltd (CPL), the Russian Foundation of Basic Research (08-02-91851 KO_a), the Royal Society, Fundação para a Ciência e Tecnologia (CERN/FP/109320/200, /116374/2010, SFRH/BPD/27054/2006, /47320/2008, /63096/200, /73676/2010), the Edinburgh Compute and Data Facilities, and SC Rosatom (H.4e.45.90.11.1059). The University of Edinburgh is a charitable body, registered in Scotland, with registration number SC005336.

REFERENCES

1. L. Reichhart, et al., *arXiv:1302.4275v1 [physics.ins-det], submitted to Astroparticle Physics* (2013).
2. D. Y. Akimov, et al., *Astroparticle Physics* **27**, 46–60 (2007).
3. V. N. Lebedenko, et al., *Physical Review D* **80**, 052010 (2009).
4. D. Y. Akimov, et al., *Physics Letters B* **709**, 14–20 (2012).
5. D. Y. Akimov, et al., *Astroparticle Physics* **34**, 151–163 (2010).
6. C. Ghag, et al., *Astroparticle Physics* **35**, 76–86 (2011).
7. A. Murphy, and S. Paling, *Nuclear Physics News* **22**, 19–24 (2012).
8. P. Antonioli, et al., *Astroparticle Physics* **7**, 357–368 (1997).
9. V. Kudryavtsev, *Computer Physics Communications* **180**, 339–346 (2009).
10. V. Kudryavtsev, N. Spooner, and J. McMillan, *Nuclear Instruments and Methods in Physics Research A* **505**, 688–698 (2003).
11. S. Agostinelli, et al., *Nuclear Instruments and Methods in Physics Research A* **506**, 250–303 (2003).
12. H. Araújo, et al., *Astroparticle Physics* **29**, 471–481 (2008).
13. A. Lindote, et al., *Astroparticle Physics* **31**, 366–375 (2009).